

Cite this: *Dalton Trans.*, 2012, **41**, 10690

www.rsc.org/dalton

PAPER

Lanthanide-ion-tuned magnetic properties in a series of three-dimensional cyano-bridged Ln^{III}W^V assemblies†Hu Zhou,^{a,b} Guo-Wang Diao,^{*a} Su-Yan Qian,^b Xiao-Zhen Yang,^b Ai-Hua Yuan,^{*c} You Song^{*d} and Yi-Zhi Li^d

Received 18th March 2012, Accepted 22nd June 2012

DOI: 10.1039/c2dt30615h

The reaction of [W(CN)₈]³⁻ with Ln³⁺ and pyrazine in acetonitrile yielded a series of isostructural compounds formulated as Ln(H₂O)₄(pyrazine)_{0.5}W(CN)₈ (Ln = La(**1**), Ce(**2**), Pr(**3**), Nd(**4**), Sm(**5**), Eu(**6**), Gd(**7**)). The Ln(III) and W(V) centers in the structure are linked through cyanide groups to form two-dimensional (2D) layers, which are further pillared by pyrazine, generating 3D frameworks. The magnetic behavior for compounds **1–7** were driven by the lanthanide ions involved. The Ln(III) and W(V) ions in compounds **2** and **5** are ferromagnetically coupled with magnetic ordering occurring at 2.8 K, comparable with magnetic ordering with the critical temperature of 1.9 K for compound **4**. In addition, the antiferromagnetic interactions were observed in compounds **3** and **7**, while no significant magnetic couplings were found in compounds **1** and **6**.

Introduction

In recent years, considerable research has been put into the design and elaboration of molecule-based magnets.¹ Of particular interest is the fact that octacyanide-bearing precursors [M(CN)₈]ⁿ⁻ (M = Mo, W with *n* = 3, 4; M = Nb with *n* = 4) are frequently utilized to construct discrete molecules, one-dimensional (1D) chains, 2D layers and 3D networks,² and the resulting materials have displayed rich magnetic properties such as high *T_c*,³ photo-/guest-induced magnetism,^{4,5} SMMs (single molecule magnets),⁶ SCMs (single chain magnets),⁷ MSHG (magnetization-induced second harmonic generation)⁸ and SCO (spin crossover) magnetism.⁹ However, [M(CN)₈]ⁿ⁻-based

4f–4d/5d assemblies that contain lanthanide ions are relatively limited and poorly investigated in comparison with the numerous 3d–4d/5d systems and [M(CN)₆]³⁻ based (M = Fe, Cr, Co, Mn) 4f–3d materials that are widely documented structurally and magnetically.^{2,10} This is because of the labilities of lanthanide ions, the rather large anisotropic magnetic moments and the absence of design strategies for 4f–4d/5d systems. In spite of this, the resulting materials have displayed unique structures¹¹ and intriguing magnetic properties, for example, long-range magnetic ordering,¹² cooling-rate-dependent magnetism¹³ and magneto-luminescent bifunction.¹⁴

It should be mentioned that rare examples of 3D octacyano-metalate-based lanthanide assemblies including [Ln(mpca)₂(H₂O)(CH₃OH)Ln(H₂O)₆W(CN)₈]*n*H₂O (Ln = Eu, Nd; Hmpca = 5-methyl-2-pyrazinecarboxylic acid)¹⁵ and [Nd^{III}(CH₃OH)₄Mo^{IV}(CN)₈]₃[Nd^{III}(H₂O)₈]·8CH₃OH¹¹ have been synthesized and characterized structurally and magnetically, in which the diamagnetic [M(CN)₈]⁴⁻ units are involved. Recently, we reported the first 3D 4f–5d compound Tb(H₂O)₄(pyrazine)_{0.5}W(CN)₈ (**8**) using 2D layers as building blocks.¹⁶ The Tb(III) and W(V) ions are coupled ferromagnetically and the reported method has provided an opportunity to obtain 3D magnets in the 4f–5d system. As is well known, the magnetic susceptibilities of lanthanide system are strongly influenced by the thermal population of sub-levels in the ground-state multiple in the ligand field.^{14b,17} Given the above considerations and as part of our ongoing efforts in the design and construction of new structural types of octacyanide-based multifunctional materials,^{16,18} our continuous interest in such systems is focused on studying the nature of magnetic exchange by varying the type of lanthanide ions involved.

In this contribution, we present a series of 3D assemblies with the general formula Ln(H₂O)₄(pyrazine)_{0.5}W(CN)₈ (Ln = La(**1**), Ce(**2**), Pr(**3**), Nd(**4**), Sm(**5**), Eu(**6**), and Gd(**7**)). Single-crystal and powder X-ray diffraction analysis revealed that compounds

^aCollege of Chemistry and Chemical Engineering, Yangzhou University, Yangzhou 225002, China. E-mail: gwldiao@yzu.edu.cn

^bSchool of Material Science and Engineering, Jiangsu University of Science and Technology, Zhenjiang 212003, China

^cSchool of Biology and Chemical Engineering, Jiangsu University of Science and Technology, Zhenjiang 212003, China. E-mail: aihuayuan@163.com

^dState Key Laboratory of Coordination Chemistry, Nanjing National Laboratory of Microstructures, School of Chemistry and Chemical Engineering, Nanjing University, Nanjing 210093, China. E-mail: yousong@nju.edu.cn

† Electronic supplementary information (ESI) available. CCDC 846239 (**4**), 866862 (**5**), 846240 (**6**), 846241 (**7**), and 866861 (**2a**) (The crystallographic data and experimental details for structural analyses for compounds **4–7** and **2a**; Selected bond lengths and angles for compounds **4–7** and **2a**; TG curve of the precursor [HN(*n*-C₄H₉)₃]₃[W(CN)₈] and compounds **1–7**; powder XRD patterns, IR spectra and EDS spectra of compounds **1–7**; powder XRD patterns of as-synthesized and simulated from single-crystal data of compound **5**, as well as simulated from single-crystal data of compound **2a**; M–H curves for compounds **2**, **4** and **5**; ac measurements for compounds **2a**, **3** and **5–7**; 1/χ_M–*T* curve, zfc–fc curve and magnetic hysteresis loop of compound **7**). For ESI and crystallographic data in CIF or other electronic format see DOI: 10.1039/c2dt30615h

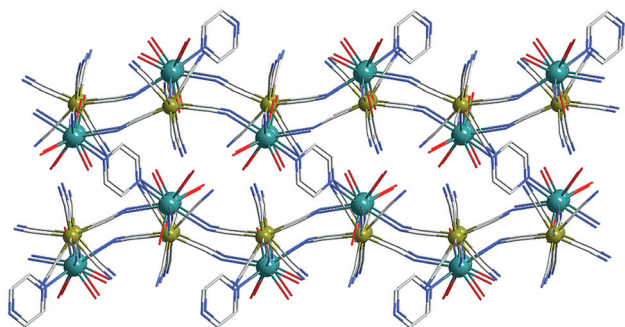


Fig. 1 The 3D framework of compounds 1–7.

1–7 are isostructural to compound 8 and exhibit a 3D open framework (Fig. 1), in which 2D corrugated layers are pillared by pyrazine ligands. It is noteworthy that the magnetic properties of compounds 1–7 were clearly driven by the lanthanide ions involved, due to ligand field effects and exchange interactions. We have previously found several systems exhibiting lanthanide-ion-induced magnetic behavior, including binuclear $[\text{Ni}^{\text{II}}\text{Ln}^{\text{III}}]$ ($\text{Ln} = \text{La}–\text{Er}$) Schiff-base compounds,¹⁹ $\text{M}(\text{CN})_6$ -based ($\text{M} = \text{Fe}, \text{Cr}$) lanthanide chains with tptz or bpy as blocking ligands (tptz = 2,4,6-tri(2-pyridyl)-1,3,5-triazine; bpy = 2,2'-bipyridine)²⁰ and cyano/bpdo mixed-bridged layers $\text{Ln}-\text{M}(\text{CN})_6$ (bpdo = 4,4'-bipyridine N,N' -dioxide; $\text{M} = \text{Fe}, \text{Co}$).²¹

Experimental

Materials and physical measurements

All chemicals and solvents were of analytical grade. The precursor $[\text{HN}(n\text{-C}_4\text{H}_9)_3]_3[\text{W}(\text{CN})_8] \cdot n\text{H}_2\text{O}$ was prepared according to the published procedure,²² and thermo-gravimetric (TG) analysis revealed that there were no crystallized water molecules (Fig. S1†). All reactions were carried out under low light conditions because of the photosensitivity of octacyanotungstate(v) ions. Elemental analyses for C, H and N were performed with a Perkin-Elmer 240C elemental analyzer. The detection of Ln and W atoms was performed with energy dispersive spectrometry (EDS, Oxford INCA). IR spectra were measured on a Nicolet FT 1703X spectrophotometer in the form of KBr pellets in the 4000–400 cm^{-1} region. Powder X-ray diffraction (XRD) patterns were collected with $\text{Cu}-\text{K}\alpha$ radiation using a Shimadzu XRD-6000 diffractometer. TG analyses were carried out at a ramp rate of 5 $^\circ\text{C min}^{-1}$ under a N_2 atmosphere using a Pyris Diamond TGA analyzer. All of the magnetization data were recorded on a Quantum Design MPMS-XL7 SQUID magnetometer. The molar magnetic susceptibilities were corrected for the diamagnetism estimated from Pascal's tables and for the sample holder by a previous calibration.²³

Syntheses of compounds $[\text{Ln}(\text{H}_2\text{O})_4(\text{pyrazine})_{0.5}][\text{W}(\text{CN})_8]$ ($\text{Ln} = \text{La}(1), \text{Ce}(2), \text{Pr}(3), \text{Nd}(4), \text{Sm}(5), \text{Eu}(6), \text{Gd}(7)$)

The products of compounds 1–7 were prepared using the reported procedure:¹⁶ the precursors $[\text{HN}(n\text{-C}_4\text{H}_9)_3]_3[\text{W}(\text{CN})_8]$ (0.20 mmol) and $\text{Ln}(\text{NO}_3)_3 \cdot 6\text{H}_2\text{O}$ (0.20 mmol) were dissolved

in acetonitrile (40 mL), and the resulting solution was stirred for 6 h. Then an acetonitrile solution (15 mL) containing pyrazine (0.60 mmol) was dropwise added into above solution at *ca.* 38 $^\circ\text{C}$. Red powders of compounds 1–7 were formed after further stirring for 24 h. The addition of excess pyrazine ligand was necessary to obtain final products with high yields. Yield for compound 1: 34.7 mg (27% based on the La salt). The other compounds (2–7) have similar mass yields. Our efforts to obtain single crystals of compounds 1–3 were unsuccessful. Single crystals of compounds 4–7 were obtained after 3 weeks by slow diffusion of an acetonitrile solution (2 mL) of pyrazine (0.15 mmol) into an acetonitrile solution (20 mL) containing $[\text{HN}(n\text{-C}_4\text{H}_9)_3]_3[\text{W}(\text{CN})_8]$ (0.05 mmol) and $\text{Ln}(\text{NO}_3)_3 \cdot 6\text{H}_2\text{O}$ (0.05 mmol). Yield for compound 4: 9.70 mg (30% based on the Nd salt). Compounds 5, 6 and 7 have similar mass yields. Powder XRD, IR, TG and EDS results (Fig. S2–S5†) indicated that as-synthesized products 1–7 and compound 8 are isostructural. Elem. anal. calcd for $\text{C}_{10}\text{H}_{10}\text{N}_9\text{O}_4\text{LaW}$ (1), %: C 18.68, H 1.57, N 19.61. Found: C 18.63, H 1.58, N 19.66. EDS (atomic ratio), $\text{La} : \text{W} = 1 : 1.02$; Elem. anal. calcd for $\text{C}_{10}\text{H}_{10}\text{N}_9\text{O}_4\text{CeW}$ (2), %: C 18.64, H 1.56, N 19.57%. Found: C 18.63, H 1.60, N 19.55. EDS, $\text{Ce} : \text{W} = 1 : 1.00$; Elem. anal. calcd for $\text{C}_{10}\text{H}_{10}\text{N}_9\text{O}_4\text{PrW}$ (3), %: C 18.62, H 1.56, N 19.54%. Found: C 18.60, H 1.59, N 19.48. EDS, $\text{Pr} : \text{W} = 1 : 0.99$; Elem. anal. calcd for $\text{C}_{10}\text{H}_{10}\text{N}_9\text{O}_4\text{NdW}$ (4), %: C 18.53, H 1.55, N 19.44. Found: C 18.36, H 1.52, N 19.58. EDS, $\text{Nd} : \text{W} = 1 : 0.97$; Elem. anal. calcd for $\text{C}_{10}\text{H}_{10}\text{N}_9\text{O}_4\text{SmW}$ (5), %: C 18.35, H 1.54, N 19.26%. Found: C 18.52, H 1.60, N 19.12. EDS, $\text{Sm} : \text{W} = 1 : 1.00$; Elem. anal. calcd for $\text{C}_{10}\text{H}_{10}\text{N}_9\text{O}_4\text{EuW}$ (6), %: C 18.31, H 1.54, N 19.22%. Found: C 18.24, H 1.50, N 19.12. EDS, $\text{Eu} : \text{W} = 1 : 0.99$; Elem. anal. calcd for $\text{C}_{10}\text{H}_{10}\text{N}_9\text{O}_4\text{GdW}$ (7), %: C 18.16, H 1.52, N 19.06%. Found: C 18.12, H 1.61, N 19.01. EDS, $\text{Gd} : \text{W} = 1 : 1.01$. IR (KBr), $\nu_{\text{C}\equiv\text{N}}$ for compound 1: 2174, 2162, 2119 cm^{-1} ; $\nu_{\text{C}\equiv\text{N}}$ for compound 2: 2176, 2160, 2118 cm^{-1} ; $\nu_{\text{C}\equiv\text{N}}$ for compound 3: 2176, 2162, 2130, 2117 cm^{-1} ; $\nu_{\text{C}\equiv\text{N}}$ for compound 4: 2178, 2168, 2158, 2118 cm^{-1} ; $\nu_{\text{C}\equiv\text{N}}$ for compound 5: 2172, 2158, 2126 cm^{-1} ; $\nu_{\text{C}\equiv\text{N}}$ for compound 6: 2180, 2171, 2160, 2125 cm^{-1} ; $\nu_{\text{C}\equiv\text{N}}$ for compound 7: 2172, 2158, 2126 cm^{-1} .

Synthesis of compound $\text{Ce}(\text{H}_2\text{O})_5\text{W}(\text{CN})_8$ (2a)

Red block-shaped single crystals of compound 2a were obtained after about 10 weeks by slow diffusion of an acetonitrile solution (2 mL) of $\text{Ce}(\text{NO}_3)_3 \cdot 6\text{H}_2\text{O}$ (0.05 mmol) into an acetonitrile solution (20 mL) containing $[\text{HN}(n\text{-C}_4\text{H}_9)_3]_3[\text{W}(\text{CN})_8]$ (0.05 mmol). Yield: 10.90 mg (35% based on the Ce salt). Elem. anal. calcd for $\text{C}_8\text{H}_{10}\text{N}_8\text{O}_5\text{CeW}$, %: C 15.44, H 1.62, N 18.01%. EDS (atomic ratio), $\text{Ce} : \text{W} = 1 : 1.00$. Found: C 15.58, H 1.61, N 18.12; IR (KBr), $\nu_{\text{C}\equiv\text{N}}$: 2175, 2162, 2117 cm^{-1} .

X-ray data collection and crystal structure refinement

Diffraction data for compounds 4–7 and 2a were collected on a Bruker Smart APEX II diffractometer equipped with $\text{Mo}-\text{K}\alpha$ ($\lambda = 0.71073 \text{ \AA}$) radiation. Diffraction data analysis and reduction were performed within *SMART*, *SAINT*, and *XPRED*.²⁴ Correction for Lorentz, polarization, and absorption effects were

performed within *SADABS*.²⁵ Structures were solved using Patterson method within *SHELXS-97* and refined using *SHELXL-97*.²⁶ All non-hydrogen atoms were refined with anisotropic thermal parameters. The H atoms of pyrazine were calculated at idealized positions and included in the refinement in a riding mode with U_{iso} for H assigned as 1.2 times U_{eq} of the attached atoms. The H atoms bound to coordinated water molecule were located from difference Fourier maps and refined as riding with $U_{\text{iso}}(\text{H}) = 1.2U_{\text{eq}}(\text{O})$. One oxygen atom coordinated to Ce1 in compound **2a** was split into two positions (O2A and O2B). The crystallographic data and experimental details for structural analyses are summarized in Table S1.† Selected bond lengths and angles are listed in Table S2.†

Results and discussion

Magnetic susceptibility measurements for compounds **1–7** and **2a** were performed on polycrystalline samples at 1000 Oe (for compounds **1**, **2**, **5**, **6**, **7** and **2a**) and 100 Oe (for compounds **3** and **4**) over the temperature range of 1.8–300 K. Let us start with the simple case of the La derivative. Compound **1** with diamagnetic La^{III} ion serves to determine the magnetic character of the low-spin W(v) ion. At 300 K, the value of $\chi_{\text{M}}T$ is 0.37 cm³ K mol⁻¹ (Fig. 2), close to the contribution of one W(v) ion (0.38 cm³ K mol⁻¹).²⁷ As the temperature is lowered, the $\chi_{\text{M}}T$ product decreases slightly and abruptly decreases at 50 K to the minimum value of 0.06 cm³ K mol⁻¹ at 1.8 K. The deviation of the magnetic susceptibility is due entirely to the anisotropy of low spin value ($S = 1/2$) of the W⁵⁺ ion. No noticeable magnetic interaction was observed in this case.

The magnetic properties of compounds **2**, **4** and **5** should be highlighted. For these compounds, the $\chi_{\text{M}}T$ curves (Fig. 3) are characterized by a continuous decrease as the temperature decreased, followed by an abrupt increase at low temperatures (below 10 K).

The room temperature $\chi_{\text{M}}T$ value (0.99 cm³ K mol⁻¹) for compound **2** is slightly lower than the theoretical value (1.18 cm³ K mol⁻¹) for the superposition of isolated Ce(III) and W(v) ions,^{17b} while the values (2.00(4) and 0.45(5) cm³ K mol⁻¹) at 300 K for compounds **4** and **5** are close to the expected

ones (2.01(4) and 0.47(5) cm³ K mol⁻¹).²⁷ The $\chi_{\text{M}}T$ values decrease continuously with cooling temperature, due to the depopulation of excited Stark sublevels, reaching minimum values of 0.60 cm³ K mol⁻¹ at 7 K, 0.73 cm³ K mol⁻¹ at 9 K, and 0.12 cm³ K mol⁻¹ at 6 K for compounds **2**, **4** and **5**, respectively. A continued decrease in the temperature leads to a sharp increase in $\chi_{\text{M}}T$, and the values of 1.39(2), 1.69(4) and 0.26(5) cm³ K mol⁻¹ were observed at 1.8 K. The abrupt increase of $\chi_{\text{M}}T$ at low temperatures indicates signals of predominant magnetic coupling between Ln(III) and W(v) centers through cyano bridge, as is well known for the ferromagnetic cyano-bridged Ln^{III}M^V (Ln = Ce, Nd, Sm; M = Mo, W) assemblies (Table 1).^{13,14b,17b,28}

The experimental field dependence of the magnetizations at 2.0(2), 1.8(4) and 2.0(5) K is shown in Fig. S6,† where the magnetization increases monotonically as the magnetic field increases and reach the values of 1.03, 1.47 and 0.39 N μ_{B} at 70 kOe for compounds **2**, **4** and **5**, respectively. These values are significantly lower than those (2.81(2), 3.90(4) and 1.71(5)) expected for the isolated-ion approximation, due to the low spin value of Ln(III) from the depopulation of excited Stark sublevels.

Compounds **2** and **5** are both characterized as ferromagnets with similar magnetic behavior at low temperatures. Isothermal magnetization experiments (Fig. 4 and 5) performed at 1.8 K exhibit a hysteresis with coercive fields of about 45(2) and 160(5) Oe, and remnant magnetizations of 0.06(2) and 0.01(5) N μ_{B} , typical of soft magnets.

Both χ' and χ'' components of ac susceptibility (Fig. 6 and Fig. S7†) present non-frequency-dependent peaks at 2.8 K, indicating the occurrence of the long-range magnetic ordering. The critical temperatures are consistent with results derived from zfc–fc data, where the zfc–fc curve showed non-reversibility and bifurcation at 2.8 K (Fig. 4 and 5, inset). The low T_{c} values for both compounds can be attributed to the universal weak coupling interactions in cyano-bridged Ln–M(CN)₆ (M = Fe, Cr) or Ln–M(CN)₈ (M = Mo, W) systems (Table 2).^{12,13,14b,20,21,29b–d}

The 2D pyrazine-free compound Ce(H₂O)₅W(CN)₈ (**2a**) has also been prepared and characterized structurally and magnetically. Single crystal X-ray diffraction analysis reveals that compound **2a** is isostructural to those materials reported previously by our group^{18c} and exhibits a 2D corrugated layered structure.

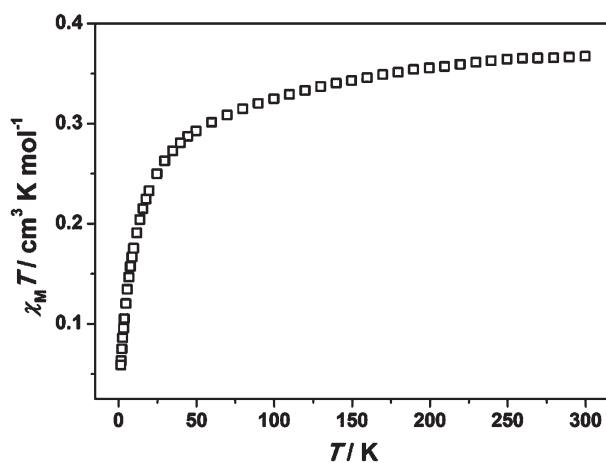


Fig. 2 Temperature dependence of $\chi_{\text{M}}T$ for compound **1**.

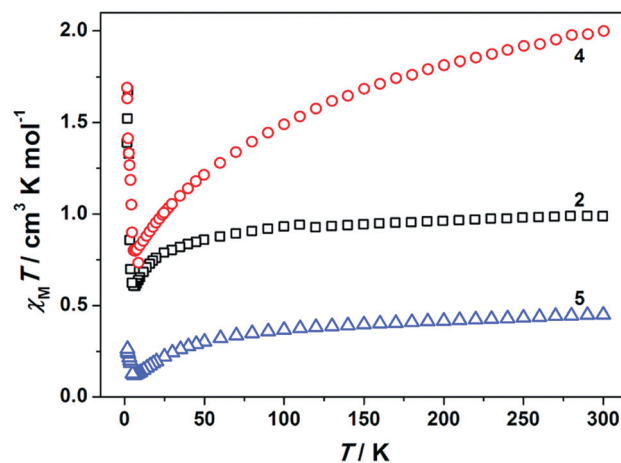
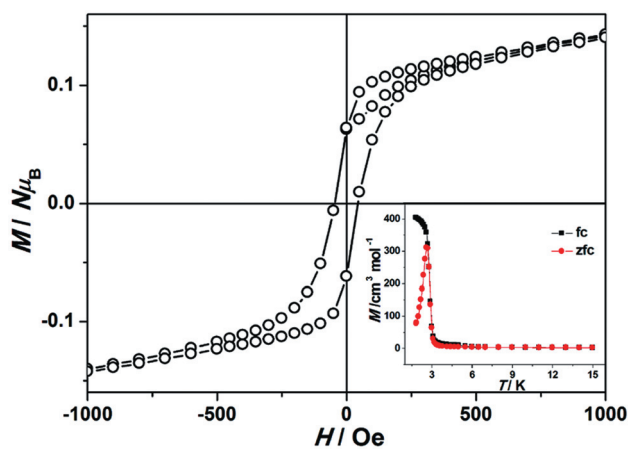
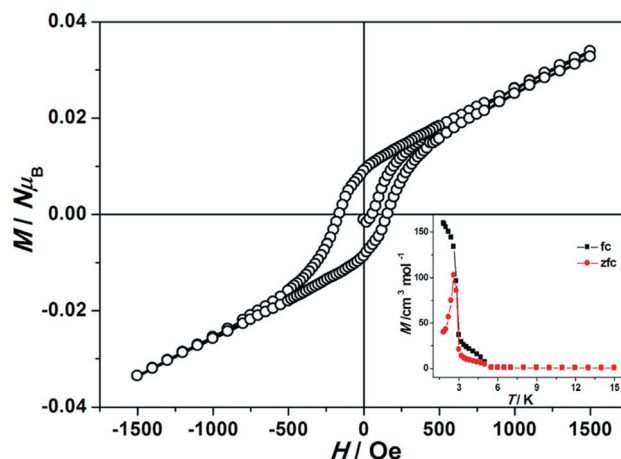


Fig. 3 Temperature dependence of $\chi_{\text{M}}T$ for compounds **2**, **4** and **5**.

Table 1 The magnetic coupling of octacyanometalate(III)-based lanthanide(III) compounds

Compounds	Structures	f^o	Magnetic properties	Ref.
CeM compounds				
Ce(pyrazine) _{0.5} (H ₂ O) ₄ W(CN) ₈ (2)	3D, hybrid network	f^2O^1	Ferromagnet, $T_c = 2.8$ K	
Ce(H ₂ O) ₅ W(CN) ₈ (2a)	2D, square grid	f^2O^0	Ferromagnet, $T_c = 2.8$ K	
{Ce ₂ (bpm)(dmf) ₈ (H ₂ O) ₂ [W(CN) ₈] ₂ } _n ·2nH ₂ O	2D, hybrid layer	f^1O^1	Ferromagnetic, $J = +1.4(3)$ cm ⁻¹	28a
[Ce ₂ (bpm)(dmsO) ₈ (H ₂ O) ₄][W(CN) ₈] ₂ ·4H ₂ O	0D, tetranuclear	f^0O^0	Ferromagnetic, $J = +1.7(2)$ cm ⁻¹	28a
[Ce ₂ (bpm)(dmf) ₆ (H ₂ O) ₈][W(CN) ₈] ₂ ·3H ₂ O	0D, ion-pair	f^0O^0	Ferromagnetic	28a
PrM compounds				
Pr(pyrazine) _{0.5} (H ₂ O) ₄ W(CN) ₈ (3)	3D, hybrid network	f^2O^1	Antiferromagnetic	
[Pr(terpy)(DMF) ₄][W(CN) ₈] ₆ ·6H ₂ O·C ₂ H ₅ OH	1D, zigzag chain	f^1O^0	Antiferromagnetic, $J = -0.07(3)$ cm ⁻¹	17b
[Pr(tmphen)(DMF) ₅][M(CN) ₈] ₂ ·DMF·2H ₂ O (M = Mo, W)	1D, helical chain	f^1O^0	Antiferromagnetic	18a
NdM compounds				
Nd(pyrazine) _{0.5} (H ₂ O) ₄ W(CN) ₈ (4)	3D, hybrid network	f^2O^1	Ferro- or ferrimagnet, $T_c = 1.9$ K	
[Nd(terpy)(DMF) ₄][W(CN) ₈] ₆ ·6H ₂ O·C ₂ H ₅ OH	1D, zigzag chain	f^1O^0	Ferromagnetic, $J = +0.47(2)$ cm ⁻¹	17b
[Nd(pzam) ₃ (H ₂ O)Mo(CN) ₈] ₂ ·H ₂ O	1D, zigzag chain	f^1O^0	Ferromagnetic, $J/k_B \approx +(1.8 \pm 0.2)$ K	28c
[Nd(phen) ₂ (DMF) ₂ (H ₂ O)Mo(CN) ₈] ₂ ·2H ₂ O	1D, zigzag chain	f^1O^0	Ferromagnetic	14a
[Nd(phen)(DMF) ₅ M(CN) ₈] ₂ ·xH ₂ O (M = Mo, W)	1D, zigzag chain	f^1O^0	Ferromagnetic	14a
SmM compounds				
Sm(pyrazine) _{0.5} (H ₂ O) ₄ W(CN) ₈ (5)	3D, hybrid network	f^2O^1	Ferromagnet, $T_c = 2.8$ K	
Sm(H ₂ O) ₅ M(CN) ₈ (M = Mo; W, 5a)	2D, square grid	f^2O^0	Ferromagnet, $T_c = 2.8-3.0$ K	13, 14b
{Sm(H ₂ O) ₉ [Sm ₂ (bpy) ₂ (OH) _{2.75} (NO ₃) _{0.25}][Mo(CN) ₈] ₂ } _n	2D, square grid	f^2O^0	Ferromagnetic, $\theta = +11.02$ K (>75 K)	28b
[Sm(terpy)(DMF) ₄][W(CN) ₈] ₆ ·6H ₂ O·C ₂ H ₅ OH	1D, zigzag chain	f^1O^0	Ferromagnetic, $J = +1.25(3)$ cm ⁻¹	17b
EuM compounds				
Eu(pyrazine) _{0.5} (H ₂ O) ₄ W(CN) ₈ (6)	3D, hybrid network	f^2O^1	Magnetically decoupled	
Eu(H ₂ O) ₅ M(CN) ₈ (M = Mo, W)	2D, square grid	f^2O^0	Antiferromagnetic	14b
[Eu(terpy)(DMF) ₄][W(CN) ₈] ₆ ·6H ₂ O·C ₂ H ₅ OH	1D, zigzag chain	f^1O^0	Magnetically decoupled	17b
GdM compounds				
Gd(pyrazine) _{0.5} (H ₂ O) ₄ W(CN) ₈ (7)	3D, hybrid network	f^2O^1	Antiferromagnetic	
Gd(H ₂ O) ₅ W(CN) ₈	2D, square grid	f^2O^0	Antiferromagnetic	14b
[Gd(terpy)(DMF) ₄][W(CN) ₈] ₆ ·6H ₂ O·C ₂ H ₅ OH	1D, zigzag chain	f^1O^0	Antiferromagnetic, $J = -1.44(3)$ cm ⁻¹	17b
[Gd(pzam) ₃ (H ₂ O)M(CN) ₈] ₂ ·H ₂ O (M = Mo, W)	1D, zigzag chain	f^1O^0	Antiferromagnetic, Mo: -0.68 cm ⁻¹ ; W: -0.76 cm ⁻¹	29a
Gd(DMA) ₅ [W(CN) ₈]	1D, zigzag chain	f^1O^0	Antiferromagnetic, $J = -0.42(1)$ cm ⁻¹	32a
Gd(DMA) ₆ [W(CN) ₈]	1D, zigzag chain	f^1O^0	Antiferromagnetic, $J = -0.28(1)$ cm ⁻¹	32a
Gd(DMF) ₆ [W(CN) ₈]	1D, zigzag chain	f^1O^0	Antiferromagnetic, $J = -0.58$ cm ⁻¹	32b
{[Gd(DMF) ₄ (MeOH) ₂][Mo(CN) ₈]} _n	1D, zigzag chain	f^1O^0	Antiferromagnetic, $\theta = -0.38$ K (>24 K)	32c

**Fig. 4** The magnetic hysteresis loop measured at 1.8 K for compound **2**. Inset: Temperature dependence of zfc and fc for compound **2** with $H = 30$ Oe.**Fig. 5** The magnetic hysteresis loop measured at 1.8 K for compound **5**. Inset: Temperature dependence of zfc and fc for compound **5** with $H = 30$ Oe.

Notably, the magnetic behavior of compound **2a** is similar to that of compound **2**, despite their different structures. For compound **2a**, a continued decrease in low temperatures (below 10 K) leads to a sharp increase in χ_{MT} (Fig. 7) and an obvious hysteresis with coercive fields of about 53 Oe and remnant magnetization of 0.20 $N\mu_B$ was observed (Fig. 8). The T_c value of

2.8 K for compound **2a** can be determined from zfc–fc (Fig. 8, inset) and ac susceptibility results (Fig. S8†).

It should be noted that just the ferromagnets $\text{Sm}(\text{H}_2\text{O})_5\text{M}(\text{CN})_8$ (M = Mo, W) and $\text{Tb}(\text{H}_2\text{O})_5\text{W}(\text{CN})_8$ were found in octacyanometalate-based lanthanide systems so far.^{13,14b} Similar

to compound **2**, the magnetic characteristics of compound **5** also resemble the corresponding 2D pyrazine-free material $\text{Sm}(\text{H}_2\text{O})_5[\text{W}(\text{CN})_8]$ (**5a**).^{13,14b} To confirm that the long-range ordering observed in compound **5** is not caused by compound **5a**, a detail comparison of powder XRD patterns was performed (Fig. S9†), which indicated that no significant impurity traces of compound **5a** were found. A very small bifurcation at 5 K for compound **5** may be due to the presence of a small proportion of an unknown phase (Fig. 5, inset). Studies into this are currently underway.

For compound **4**, the isothermal magnetization experiment (Fig. 9) performed at 1.8 K exhibits a hysteresis with a coercive field of 47 Oe and a small remnant magnetization of $0.006 \text{ N}\mu_{\text{B}}$, suggesting that compound **4** behaves as a magnet. The χ' and χ'' components (Fig. 9, inset) of the ac susceptibility increased rapidly at low temperatures and reached the maximum at 1.9 K, being the onset of the long-range ordering with the critical temperature of 1.9 K. Obviously, the exact coupling nature (ferri- or ferromagnets) for compound **4** can not be determined based on the above experiments.

The observed $\chi_{\text{M}}T$ values (Fig. 10) at 300 K for compounds **3** and **6** are equal to 2.37 and $1.42 \text{ cm}^3 \text{ K mol}^{-1}$, respectively, which are inconsistent with those ($1.98(3)$ and $1.88(6) \text{ cm}^3 \text{ K mol}^{-1}$)

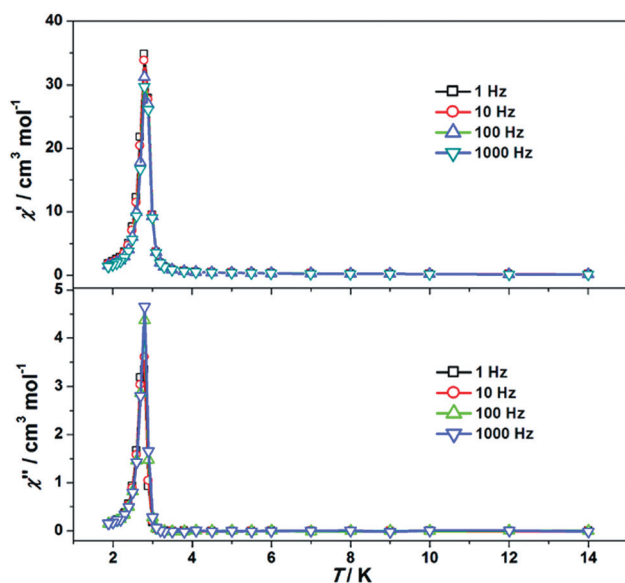


Fig. 6 Temperature dependence of the ac susceptibility for compound **2** at different frequencies under $H_{\text{ac}} = 3.5 \text{ Oe}$ and $H_{\text{dc}} = 0 \text{ Oe}$.

expected for the isolated Ln^{III} and W^{V} ions, due to the depopulation of excited Stark sublevels of $\text{Ln}(\text{III})$.^{14b,17b,18a} Upon cooling, the $\chi_{\text{M}}T$ products decrease monotonically to the minimum values of $0.15(3)$ and $0.06(6) \text{ cm}^3 \text{ K mol}^{-1}$ at 1.8 K. As shown in Fig. S10,† the magnetizations for both compounds at 2.0 K increase monotonically with an increasing value of the magnetic field and reach the values of $0.41(3)$ at 70 kOe and $0.15(6) \text{ N}\mu_{\text{B}}$ at 60 kOe, which are significantly lower than those expected for

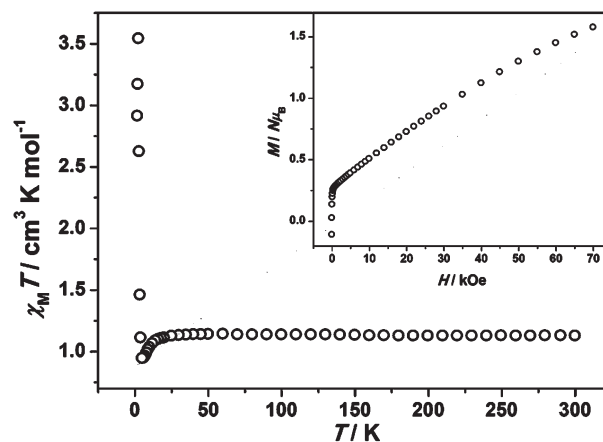


Fig. 7 Temperature dependence of $\chi_{\text{M}}T$ for compound **2a**. Inset: Field dependence of the magnetization for compound **2a**.

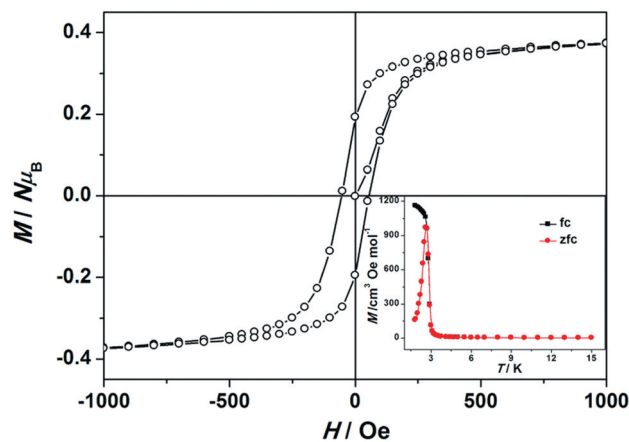


Fig. 8 The magnetic hysteresis loop measured at 1.8 K for compound **2a**. Inset: Temperature dependence of zfc and fc for compound **2a** with $H = 30 \text{ Oe}$.

Table 2 Octa- and hexacyanometalate-based lanthanide compounds with low T_{c} values

Compounds	Structures	T_{c} values	Ref.
$[\text{Tb}(\text{pzam})_3(\text{H}_2\text{O})\text{Mo}(\text{CN})_6] \cdot \text{H}_2\text{O}$	1D, zigzag chain	1.0 K	12
$\text{Sm}(\text{H}_2\text{O})_5\text{M}(\text{CN})_8$ (M = Mo, W)	2D, square grid	2.8–3.0 K	13, 14b
$\{\text{Sm}(\text{tptz})(\text{H}_2\text{O})_4\text{Fe}(\text{CN})_6\}_\infty \cdot 8\text{H}_2\text{O}$ (tptz = 2,4,6-tri(2-pyridyl)-1,3,5-triazine)	1D, linear chain	3.5 K	20a
$\text{trans}-[\text{Cr}(\text{CN})_4(\mu\text{-CN})_2\text{Sm}(\text{H}_2\text{O})_4(\text{bpy})]_n \cdot 3.5n\text{H}_2\text{O} \cdot 1.5n\text{bpy}$	1D, chain	<2.0 K	20b
$\{\{\text{Ln}(\text{bpdo})(\text{H}_2\text{O})_2\text{Fe}(\text{CN})_6\} \cdot 2\text{H}_2\text{O}\}_n$ (Ln = Sm, Gd; bpdo = 4,4'-bipyridine N, N'-dioxide)	2D, square grid	Sm: 2.9 K; Gd: 1.9 K	21
$\text{trans}-[\text{Fe}(\text{CN})_4(\mu\text{-CN})_2\text{Dy}(\text{H}_2\text{O})_4(\text{bpy})]_n \cdot 4n\text{H}_2\text{O} \cdot 1.5n\text{bpy}$	1D, chain	2.5 K	29b
$\text{trans}-[\text{Fe}(\text{CN})_4(\mu\text{-CN})_2\text{Sm}(\text{H}_2\text{O})_4(\text{bpy})]_n \cdot 5n\text{H}_2\text{O} \cdot 1.5n\text{bpy}$	1D, chain	3.5 K	29c
$[\text{Sm}(\text{DMF})_2(\text{H}_2\text{O})_3\text{Cr}(\text{CN})_6] \cdot \text{H}_2\text{O}$	2D, brick wall-like layer	4.2 K	29d

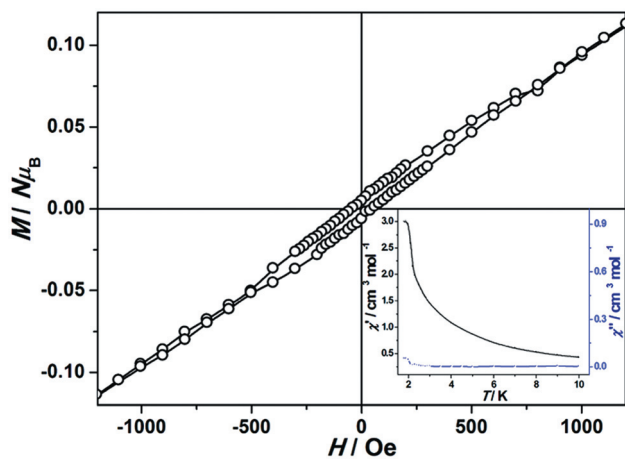


Fig. 9 The hysteresis loop measured at 1.8 K for compound 4. Inset: Temperature dependence of the ac susceptibility for compound 4 at 10 Hz under $H_{ac} = 5$ Oe and $H_{dc} = 0$ Oe.

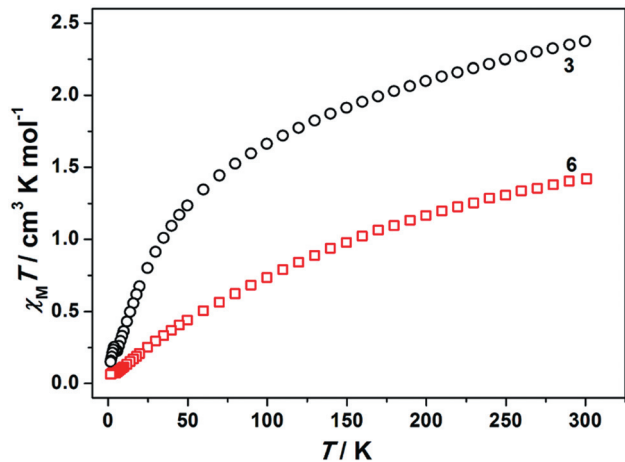


Fig. 10 Temperature dependence of $\chi_M T$ for compounds 3 and 6.

the isolated-ion approximation, due to the low spin value of Ln(III).

To detect the magnetic behavior at low temperatures, ac measurements for both compounds were performed. Unfortunately, the χ' component of ac susceptibility for compound 3 remains unchanged down to 1.8 K, while no signal was observed in the χ'' component (Fig. S11†). Furthermore, both components showed no frequency-dependence in the frequency range of 1 to 1 kHz. Based on the above experiments, we can conclude that the Pr(III) and W(V) ions in compound 3 are antiferromagnetically coupled, which is comparable to the results observed in other cyano-bridged Pr^{III}W^V assemblies [Pr(terpy)(DMF)₄][W(CN)₈]₆H₂O·C₂H₅OH ($J = -0.07(3)$ cm⁻¹; terpy = 2,2':6',2''-terpyridine)^{17b} and [Pr(tmphen)(DMF)₅][W(CN)₈]₆DMF·2H₂O (tmphen = 3,4,7,8-tetramethyl-1,10-phenanthroline).^{18a}

The Eu^{III} ion has a non-magnetic ground state, so the low-temperature magnetic behavior for compound 6 should be defined by exchange interactions only W–CN–Eu–NC–W bridge.³⁰ The magnetic character observed at low temperature may be attributed to non-magnetic ground level of Eu(III) and the

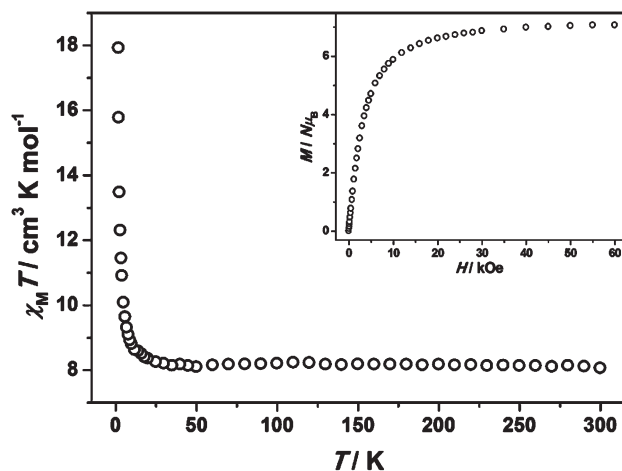


Fig. 11 Temperature dependence of $\chi_M T$ for compound 7. Inset: Field dependence of the magnetization for compound 7.

weak antiferromagnetic coupling between the W(V) units. Lariovna and co-workers reported the antiferromagnetic compounds [Eu(H₂O)₅][M(CN)₈] (M = Mo, W), in which the χ' component of ac susceptibility showed a frequency-independent peak at 2.33 K.^{14b} However, the χ' component in our case remained unchanged as temperature decreases and increases slightly below 4 K, while no signals were observed in the χ'' component (Fig. S12†). So the Eu(III) and W(V) centers in compound 6 are magnetically uncoupled, fitting nicely with the other Eu^{III}W^V compound [Eu(terpy)(DMF)₄][W(CN)₈]₆H₂O·C₂H₅OH.^{17b}

The $\chi_M T$ value (Fig. 11) of 8.06 cm³ K mol⁻¹ at 300 K for compound 7 is lower slightly than the expected value of 8.25 cm³ K mol⁻¹ for isolated one Gd^{III} and one W^V.^{17b,31} Below 110 K, the $\chi_M T$ value decreased slightly by lowering temperatures to reach the minimum value of 8.09 cm³ K mol⁻¹ at 50 K. The Gd^{III} ion has a ⁸S_{7/2} ground state without first-order angular momentum. In the absence of crystal field effects, the decrease of $\chi_M T$ value at high temperatures is characteristic of antiferromagnetic interactions between Gd(III) and W(V) ions. Upon further cooling, a sharp increase was observed with the maximum value of 17.91 cm³ K mol⁻¹ at 1.8 K. The temperature dependence (Fig. S13†) of $1/\chi_M$ above 50 K obeys the Curie–Weiss law with a negative Weiss constant $\theta = -1.26$ K, further suggesting the existence of the antiferromagnetic coupling between spin carriers. The magnetic behavior observed in compound 7 is consistent with several 1D cyano-bridged Gd^{III}M^V (M = Mo, W) compounds with negative J (or θ) values (Table 1).^{17b,29a,32}

The field dependence of the magnetization (Fig. 11, inset) for compound 7 measured at 2.0 K shows a rapid increase to 6.10 N_B at 12 kOe, then gradually to the saturation values of 7.06 N_B at 60 kOe, which is between antiferromagnetic (6 N_B) and ferromagnetic (8 N_B) Gd(III)–W(V) interactions through the cyano bridge. This behavior indicates the easy reversal of local spins from initial antiparallel to parallel against the antiferromagnetic coupling between Gd(III) and W(V) ions.^{30b}

To explore the dynamics of magnetization at low temperature, ac magnetic measurements were performed (Fig. S14†).

Different slightly from the results found in 2D pyrazine-free materials $\text{Gd}(\text{H}_2\text{O})_5\text{M}(\text{CN})_8$ ($\text{M} = \text{Mo}, \text{W}$),^{14b} the χ' component of compound **7** increased monotonically as temperature decreased and increased rapidly below 4 K, whereas no signal was observed in the χ'' component. Both χ' and χ'' components showed no frequency-dependence in the frequencies range between 1 and 1 kHz. In addition, the magnetization in the zfc–fc curve (Fig. S15†) revealed complete reversibility and no magnetic hysteresis loop was detected (Fig. S16†). The above experimental results suggest the absence of long-range magnetic ordering for compound **7** at low temperature. Further analysis was hampered due to temperature limitations of the low-temperature apparatus.

In order to investigate the factors affecting magnetic properties of octacyanometalate-based lanthanide (4f–4d/5d) systems, we compared the magnetic coupling of compounds **1–7** with those of related materials reported previously (Table 1). The comparative results revealed that magnetic behavior for 4f–4d/5d systems were driven by the lanthanide ions involved. Generally, ferromagnetic interactions were observed for LnM ($\text{Ln} = \text{Ce}, \text{Nd}, \text{Sm}$) compounds and antiferromagnetic for LnM ($\text{Ln} = \text{Pr}, \text{Eu}, \text{Gd}$) compounds.

According to Cheetham,³³ octacyanometalate-based lanthanide systems can be classified using I^xO^y symbols, where x and y denoted the dimensionality of the inorganic (I) and organic (O) subnetworks, respectively. We can see from Table 1 that the magnetic properties of 4f–4d/5d systems comprising of the same lanthanide ions were tuned slightly by cyano-bridged skeletons (inorganic subnetworks) in the structures. For 2D pyrazine-free layers $\text{Ln}(\text{H}_2\text{O})_5\text{W}(\text{CN})_8$ (I^2O^0) and 3D hybrid systems (I^2O^1) (**1–7**) in our case, the inorganic subnetworks (Ln–NC–W linkages) are similar despite the different dimensionalities of both series. In fact, the similarity in the magnetic behavior of compounds **2** (or **5**) and **2a** (or **5a**) could also be expected if one takes into account the established weak influence of organic linker between the cyanide-bridged frameworks observed in other $\text{Ln}^{\text{III}}\text{W}^{\text{V}}$ systems, in which the rather weak and antiferromagnetic exchange coupling mediated through the 2,2'-bipyrimidine (bpm) ligand, compared to the more effective and ferromagnetic coupling between the Ce^{III} and W^{V} ions linked by the cyanide bridge.^{28a}

The above results showed that magnetic properties for 3D hybrid materials (**1–7**) depend mainly on the introduction of $\text{Ln}\cdots\text{W}$ interactions through cyanide bridges, and pyrazine has a minor effect on the magnetic results. We assign the presence of magnetic ordering in compounds **2**, **4** and **5** mainly to the effective ferromagnetic $\text{Ln}^{\text{III}}\text{–W}^{\text{V}}$ coupling through cyanide bridges. From this perspective, the inorganic–organic hybrid materials (**1–7**) present in this contribution should be structurally 3D but only magnetically 2D.

Conclusion

A series of isostructural 3D octacyanotungstate(v)-based lanthanide compounds (**1–7**) have been synthesized through the self-assembly reaction between $[\text{W}(\text{CN})_8]^{3-}$, Ln^{3+} and pyrazine in acetonitrile. These compounds are rare examples of 3D architectures constructed from octacyanometalates and lanthanide

ions, and the magnetic properties have been tuned by changing lanthanide ions involved. Most importantly, compounds **2**, **4** and **5** represent the first magnets with 3D networks for a octacyanometalate-based lanthanide system. The magnetic results of 2D pyrazine-free compounds $\text{Ln}(\text{H}_2\text{O})_5\text{M}(\text{CN})_8$ and 3D inorganic–organic hybrid materials (**1–7**) confirmed the dominant and more effective cyano-mediated $\{\text{Ln–NC–W}\}$ interaction, compared to the rather weak $\{\text{Ln–pyrazine–Ln}\}$ coupling mediated through the spacer ligand pyrazine. Consistent magnetic behavior for both series can be attributed to the similarity of CN-bridged skeletons (inorganic subnetworks) in the structures. Studies in this field are underway in our laboratory.

Acknowledgements

This research was supported by the National Natural Science Foundation (51072072, 51102119, 20973151, 91022031), the Natural Science Foundation of Jiangsu Province (BK2010343, BK2011518), and the Fundamental Research Funds for the Central Universities (1093020504). The authors thank Zhu-Guo Chang and Dr Bin Liu (Northwest University, China) for the magnetic measurements. The authors are also grateful to Dr Hong-Bo Zhou (Jiangsu University, China) for useful magnetic discussions.

References

- J. S. Miller and D. Gatteschi, *Chem. Soc. Rev.*, 2011, **40**, 3065.
- B. Sieklucka, R. Podgajny, T. Korzeniak, B. Nowicka, D. Pinkowicz and M. Koziel, *Eur. J. Inorg. Chem.*, 2011, 305.
- (a) T.-W. Wang, J. Wang, S. Ohkoshi, Y. Song and X.-Z. You, *Inorg. Chem.*, 2010, **49**, 7756; (b) W. Kosaka, K. Imoto, Y. Tsunobuchi and S. Ohkoshi, *Inorg. Chem.*, 2009, **48**, 4604; (c) D. Pinkowicz, R. Podgajny, M. Bałanda, M. Makarewicz, B. Gaweł, W. Łasocha and B. Sieklucka, *Inorg. Chem.*, 2008, **47**, 9745; (d) J. M. Herrera, P. Franz, R. Podgajny, M. Pilkington, M. Biner, S. Decurtins, H. Stoeckli-Evans, A. Neels, R. Garde, Y. Dromzée, M. Julve, B. Sieklucka, K. Hashimoto, S. Ohkoshi and M. Verdager, *C. R. Chim.*, 2008, **11**, 1192; (e) R. Podgajny, D. Pinkowicz, T. Korzeniak, W. Nitek, M. Rams and B. Sieklucka, *Inorg. Chem.*, 2007, **46**, 10416; (f) J.-Z. Zhong, H. Seino, Y. Mizobe, M. Hidai, M. Verdager, S. Ohkoshi and K. Hashimoto, *Inorg. Chem.*, 2000, **39**, 5095.
- (a) F. Volatron, D. Heurtaux, L. Catala, C. Mathonière, A. Gloter, O. Stéphane, D. Repetto, M. Clemente-León, E. Coronado and T. Mallah, *Chem. Commun.*, 2011, **47**, 1985; (b) W. Zhang, H.-L. Sun and O. Sato, *Dalton Trans.*, 2011, **40**, 2735; (c) H.-H. Zhao, M. Shatruk, A. V. Prosvirin and K. R. Dunbar, *Chem.–Eur. J.*, 2007, **13**, 6573; (d) S. Ohkoshi, S. Ikeda, T. Hozumi, T. Kashiwagi and K. Hashimoto, *J. Am. Chem. Soc.*, 2006, **128**, 5320; (e) S. Ohkoshi, H. Tokoro, T. Hozumi, Y. Zhang, K. Hashimoto, C. Mathonière, I. Bord, G. Rombaut, M. Verelst, C. C. dit Moulin and F. Villain, *J. Am. Chem. Soc.*, 2006, **128**, 270; (f) C. Mathonière, R. Podgajny, P. Guionneau, C. Labrugere and B. Sieklucka, *Chem. Mater.*, 2005, **17**, 442; (g) T. Hozumi, K. Hashimoto and S. Ohkoshi, *J. Am. Chem. Soc.*, 2005, **127**, 3864; (h) J. M. Herrera, V. Marvaud, M. Verdager, J. Marrot, M. Kalisz and C. Mathonière, *Angew. Chem., Int. Ed.*, 2004, **43**, 5468; (i) Y. Arimoto, S. Ohkoshi, Z.-J. Zhong, H. Seino, Y. Mizobe and K. Hashimoto, *J. Am. Chem. Soc.*, 2003, **125**, 9240.
- (a) D. Pinkowicz, R. Podgajny, B. Gaweł, W. Nitek, W. Łasocha, M. Oszajca, M. Czapla, M. Makarewicz, M. Bałanda and B. Sieklucka, *Angew. Chem., Int. Ed.*, 2011, **50**, 3973; (b) R. Podgajny, S. Choraży, W. Nitek, A. Budziak, M. Rams, C. J. Gómez-García, M. Oszajca, W. Łasocha and B. Sieklucka, *Cryst. Growth Des.*, 2011, **11**, 3866; (c) B. Nowicka, M. Bałanda, B. Gaweł, G. Ćwiak, A. Budziak, W. Łasocha and B. Sieklucka, *Dalton Trans.*, 2011, **40**, 3067; (d) M. Koziel, R. Podgajny, R. Kania, R. Lebris, C. Mathonière,

- K. Lewiński, K. Kruczała, M. Rams, C. Labrugère, A. Bousseksou and B. Sieklucka, *Inorg. Chem.*, 2010, **49**, 2765.
- 6 (a) M. G. Hilfinger, H.-H. Zhao, A. Prosvirin, W. Wernsdorfer and K. R. Dunbar, *Dalton Trans.*, 2009, 5155; (b) J. H. Lim, J. H. Yoon, H. C. Kim and C. S. Hong, *Angew. Chem., Int. Ed.*, 2006, **45**, 7424; (c) Y. Song, P. Zhang, X.-M. Ren, X.-F. Shen, Y.-Z. Li and X.-Z. You, *J. Am. Chem. Soc.*, 2005, **127**, 3708.
- 7 (a) T. S. Venkatakrisnan, S. Sahoo, N. Bréfuel, C. Duhayon, C. Paulsen, A. Barra, S. Ramasesha and J.-P. Sutter, *J. Am. Chem. Soc.*, 2010, **132**, 6047; (b) J. H. Yoon, D. W. Ryu, S. Y. Choi, H. C. Kim, E. K. Koh, J. Tao and C. S. Hong, *Chem. Commun.*, 2011, **47**, 10416.
- 8 D. Pinkowicz, R. Podgajny, W. Nitek, M. Rams, A. M. Majcher, T. Nuida, S. Ohkoshi and B. Sieklucka, *Chem. Mater.*, 2011, **23**, 21.
- 9 (a) S. Ohkoshi, K. Imoto, Y. Tsunobuchi, S. Takano and H. Tokoro, *Nat. Chem.*, 2011, **3**, 564; (b) M. Arai, W. Kosaka, T. Matsuda and S. Ohkoshi, *Angew. Chem., Int. Ed.*, 2008, **47**, 6885.
- 10 (a) M. Andruh, J. P. Costes, C. Diaz and S. Gao, *Inorg. Chem.*, 2009, **48**, 3342; (b) S. Tanase and J. Reedijk, *Coord. Chem. Rev.*, 2006, **250**, 2501.
- 11 Z.-X. Wang, X.-F. Shen, J. Wang, P. Zhang, Y.-Z. Li, E. N. Nfor, Y. Song, S. Ohkoshi, K. Hashimoto and X.-Z. You, *Angew. Chem., Int. Ed.*, 2006, **45**, 3287.
- 12 F. Prins, E. Pasca, L. J. de Jongh, H. Kooijman, A. L. Spek and S. Tanase, *Angew. Chem., Int. Ed.*, 2007, **46**, 6081.
- 13 T. Hozumi, S. Ohkoshi, Y. Arimoto, H. Seino, Y. Mizobe and K. Hashimoto, *J. Phys. Chem. B*, 2003, **107**, 11571.
- 14 (a) J. Long, E. Chelebaeva, J. Larionova, Y. Guari, R. A. S. Ferreira, L. D. Carlos, F. A. A. Paz, A. Trifonov and C. Guérin, *Inorg. Chem.*, 2011, **50**, 9924; (b) E. Chelebaeva, J. Larionova, Y. Guari, R. A. S. Ferreira, L. D. Carlos, F. A. A. Paz, A. Trifonov and C. Guérin, *Inorg. Chem.*, 2009, **48**, 5983; (c) E. Chelebaeva, J. Larionova, Y. Guari, R. A. S. Ferreira, L. D. Carlos, F. A. A. Paz, A. Trifonov and C. Guérin, *Inorg. Chem.*, 2008, **47**, 775.
- 15 S. Tanase, F. Prins, J. M. M. Smits and R. de Gelder, *CrystEngComm*, 2006, **8**, 863.
- 16 H. Zhou, A.-H. Yuan, S.-Y. Qian, Y. Song and G.-W. Diao, *Inorg. Chem.*, 2010, **49**, 5971.
- 17 (a) S. Tanase, M. Ferbinteanu and F. Cimpoesu, *Inorg. Chem.*, 2011, **50**, 9678; (b) P. Przychodzeń, R. Pelka, K. Lewiński, J. Supel, M. Rams, K. Tomala and B. Sieklucka, *Inorg. Chem.*, 2007, **46**, 8924.
- 18 (a) S.-Y. Qian, H. Zhou, A.-H. Yuan and Y. Song, *Cryst. Growth Des.*, 2011, **11**, 5676; (b) A.-H. Yuan, S.-Y. Qian, W.-Y. Liu, H. Zhou and Y. Song, *Dalton Trans.*, 2011, **40**, 5302; (c) A.-H. Yuan, P. D. Southon, D. J. Price, C. J. Kepert, H. Zhou and W. Y. Liu, *Eur. J. Inorg. Chem.*, 2010, 3610.
- 19 T. D. Pasatoiu, J.-P. Sutter, A. M. Madalam, F. Z. C. Fella, C. Duhayon and M. Andruh, *Inorg. Chem.*, 2011, **50**, 5890.
- 20 (a) H.-H. Zhao, N. Lopez, A. Prosvirin, H. T. Chifotides and K. R. Dunbar, *Dalton Trans.*, 2007, 878; (b) M. Estrader, J. Ribas, V. Tangoulis, X. Solans, M. Font-Bardía, M. Maestro and C. Diaz, *Inorg. Chem.*, 2006, **45**, 8239.
- 21 Y.-Z. Zhang, G.-P. Duan, O. Sato and S. Gao, *J. Mater. Chem.*, 2006, **16**, 2625.
- 22 L. D. C. Bok, J. G. Leipoldt and S. S. Basson, *Z. Anorg. Allg. Chem.*, 1975, **415**, 81.
- 23 O. Kahn, *Molecular Magnetism*, VCH Publisher, New York, 1993.
- 24 Bruker, *SMART, SAINT and XPREP: Area Detector Control and Data Integration and Reduction Software*, Bruker Analytical X-ray Instruments Inc., Madison, Wisconsin, USA, 1995.
- 25 G. M. Sheldrick, *SADABS: Empirical Absorption and Correction Software*, University of Göttingen, Göttingen, Germany, 1996.
- 26 (a) G. M. Sheldrick, *SHELXS-97. Program for X-ray Crystal Structure Determination*, Göttingen University, Göttingen, Germany, 1997; (b) G. M. Sheldrick, *SHELXL-97. Program for X-ray Crystal Structure Determination*, Göttingen University, Göttingen, Germany, 1997; (c) G. M. Sheldrick, *Acta Crystallogr., Sect. A: Found. Crystallogr.*, 2008, **64**, 112.
- 27 R. L. Carlin, *Magnetochemistry*, Springer, Berlin, 1997.
- 28 (a) M. Koziel, R. Pelka, M. Rams, W. Nitek and B. Sieklucka, *Inorg. Chem.*, 2010, **49**, 4268; (b) S.-L. Ma, S. Ren, Y. Ma and D.-Z. Liao, *J. Chem. Sci.*, 2009, **121**, 421; (c) S. Tanase, M. Evangelisti, L. J. de Jongh, J. M. M. Smits and R. de Gelder, *Inorg. Chim. Acta*, 2008, **361**, 3548.
- 29 (a) S. Tanase, L. J. De Jongh, F. Prins and M. Evangelisti, *Chem-PhysChem*, 2008, **9**, 1975; (b) A. Figuerola, J. Ribas, D. Casanova, M. Maestro, S. Alvarez and C. Diaz, *Inorg. Chem.*, 2005, **44**, 6949; (c) A. Figuerola, C. Diaz, J. Ribas, V. Tangoulis, C. Sangregorio, D. Gatteschi, M. Maestro and J. Mahía, *Inorg. Chem.*, 2003, **42**, 5274; (d) H.-Z. Kou, S. Gao and X.-L. Jin, *Inorg. Chem.*, 2001, **40**, 6295.
- 30 (a) E. N. Chelebaeva, A. A. Trifonov, J. E. Larionova, Y. Guari, R. A. S. Ferreira, L. D. Carlos, F. A. A. Paz and C. Guérin, *Russ. Chem. Bull.*, 2010, **59**, 476; (b) C. Benelli, A. Caneschi, D. Gatteschi, L. Pardi and P. Rey, *Inorg. Chem.*, 1989, **28**, 275.
- 31 P. Przychodzeń, K. Lewiński, R. Pelka, M. Bałanda, K. Tomala and B. Sieklucka, *Dalton Trans.*, 2006, 625.
- 32 (a) W. Kosaka, K. Hashimoto and S. Ohkoshi, *Bull. Chem. Soc. Jpn.*, 2007, **80**, 2350; (b) S. Ikeda, T. Hozumi, K. Hashimoto and S. Ohkoshi, *Dalton Trans.*, 2005, 2120; (c) S.-L. Ma, Y. Ma, D.-Z. Liao, S.-P. Yan, Z.-H. Jiang and G.-L. Wang, *Chin. J. Inorg. Chem.*, 2008, **24**, 1290.
- 33 A. K. Cheetham, C. N. R. Rao and R. K. Feller, *Chem. Commun.*, 2006, 4780.